Water Oxidation

DOI: 10.1002/anie.201207215

Copper(II) Catalysis of Water Oxidation**

*Zuofeng Chen and Thomas J. Meyer**

As the terminal step in Photosystem II (PSII), and a potential half-reaction for artificial photosynthesis, water oxidation ($2H_2O \rightarrow O_2 + 4H^+ + 4e^-$) is a key reaction, but it imposes a significant mechanistic challenge in its requirements for both $4e^-/4H^+$ loss and O–O bond formation. Rapid progress has recently been made based with single site polypyridyl Ru[1–4] and Ir[5–7] complexes, pre-prepared Mn oxide clusters,[8] Co and Ni clusters that spontaneously form in solution,[9,10] Co_3O_4 (spinel) particles,[11] cobalt-based polyoxometallates,[12,13] colloidal $IrO_2 \cdot n H_2O$,[14] amorphous iridium oxide deposited from organometallic precursors,[15] and, most recently, copper-bipyridine complexes.[16] There is a continuing need for stable, rapid, and easily accessible catalysts for this reaction, ideally based on earth-abundant elements.

Cu^{II} has both a well-defined coordination chemistry and an extensive redox chemistry based on reduction to Cu^0 and Cu^I, and oxidation to Cu^{III} or even Cu^{IV}.[17–24] With a propensity for square-planar coordination, d^8 Cu^{III} is found as an intermediate in reactions of organocopper compounds and in bis(μ-oxo)-bridged complexes.[17–19,22–24] Cu^{IV} complexes stabilized either by fluoride ligands or as linear O=Cu=O are also known.[20,21] Copper complexes of higher oxidation state have been shown to oxidize phenols, alcohols, and even hydrocarbons.[22–24] We report here that, under appropriate conditions, simple Cu^{II} salts at a variety of electrodes are highly active in electrocatalytic water oxidation.

Figure 1 a shows cyclic voltammograms (CVs) obtained at a boron-doped diamond (BDD) electrode (0.071 cm^2) with the addition of increasing amounts of $CuSO_4$ in Na_2CO_3 solution (1 M, pH = ca. 10.8) aqueous solutions. In the absence of $CuSO_4$ at potentials < 1.45 V vs. the normal hydrogen electrode (NHE), only small double layer charging currents were observed, with no significant Faradaic component. A small background oxygen evolution current at the BDD electrode begins at about 1.45 V under these conditions. With Cu^{II} added as $CuSO_4$, a dramatic current enhancement is observed above background. The onset potential ($E_{p,o}$) for water oxidation and the potential at the oxidative current

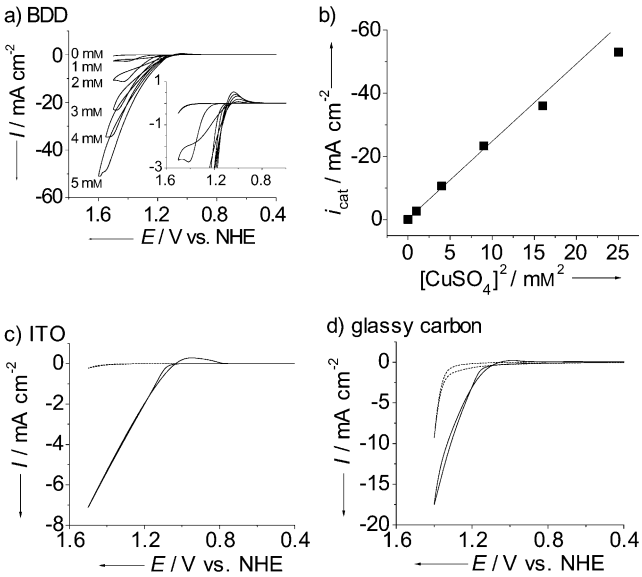

Figure 1. a) CVs in Na_2CO_3 solution (1 M, pH = ca. 10.8) at a BDD electrode (0.071 cm^2) with increasing amounts of added $CuSO_4$, as noted in the figure. The inset shows magnified views of the catalytic current response for reverse scans. b) Plot of catalytic peak/plateau current density i_{cat} vs. $[Cu^{II}]^2$. c) As in (a), but at an ITO electrode (0.70 cm^2); a similar result was obtained at an FTO electrode. d) As in (a), but at a glassy carbon electrode (0.071 cm^2). Scan rate = 100 $mV s^{-1}$, temperature = 22 °C.

peak/plateau ($E_{p,a}$) vary slightly with the concentration of added Cu^{II}. The former appears at ca. 1.05 V, with an overpotential of ca. 0.45 V, and the latter at ca. 1.46 V with 3 mM of added Cu^{II}, with a peak current density reaching ca. 23 mA cm^{-2}. This is ca. 2.5 times higher than the maximum current densities achieved for a recently reported copper-bipyridine catalyst under comparable conditions (pH 12.5) with similar over potentials. Current densities for the latter were limited by kinetic saturation above 0.5 mM catalyst loading.[16]

No additional peak/plateau features are observed with further scanning up to 1.90 V (Supporting Information, Figure S1). In the reverse scan, a current crossover appears along with a small re-reduction wave at $E_{p,c}$ = ca. 1.02 V ($E_{p,c}$ = reductive peak/plateau potential). The appearance of this feature is consistent with re-oxidation of an intermediate, presumably a peroxide species, which undergoes reduction at a more negative potential (see below for further discussion).

The catalytic peak/plateau current density (i_{cat}) for water oxidation is relatively independent of the scan rate from 10–100 mV s^{-1} (compare with the diffusion-limited $[Fe^{III}(CN)_6]^{3-}/[Fe^{II}(CN)_6]^{4-}$ couple in Figure S2). The lack of a significant scan rate dependence is consistent with rate limiting water oxidation at the electrode. Under these

[*] Dr. Z.-F. Chen, Prof. T. J. Meyer
Department of Chemistry, University of North Carolina at Chapel Hill, Chapel Hill, NC 27599 (USA)
E-mail: tjmeyer@unc.edu

[**] Funding by the UNC Energy Frontier Research Center (EFRC) for Solar Fuels, an EFRC funded by the U.S. Department of Energy, Office of Science, Office of Basic Energy Sciences (DE-SC0001011, supporting Z.-F.C. for the electrochemical experiments), and the Army Research Office (W911NF-09-1-0426, supporting Z.-F.C. for product analysis), is gratefully acknowledged. We thank Prof. R. W. Murray for helpful discussions.

Supporting information for this article, including experimental details, is available on the WWW under http://dx.doi.org/10.1002/anie.201207215.

conditions, i_{cat} varies linearly with $[Cu^{II}]^2$ up to ca. 3 mM (Figure 1b).[25] The deviation from linearity above 3 mM, up to the limit of Cu^{II} solubility at 5 mM, may be an artifact arising from the loss of effective surface area owing to oxygen gas bubble formation. The latter is easily observable, even during single CV scans at 100 mV s^{-1} (Figure S3).

CV waveforms were sustainable and reproducible for at least six series of 25 continuous scan cycles (Figure S4). During initial scans, the current density decreased as gas bubbles accumulated on the electrode surface, but the current response stabilized in subsequent cycles and initial current responses were largely recovered by agitation to remove gas bubbles from the surface. As the number of scans was increased, the initial peak current density in each series was largely unchanged, with less than 10% variation. These observations point to intrinsic solution kinetics with a dependence of i_{cat} on $[Cu^{II}]^2$, and di-Cu catalysis.

Similar results were obtained with the salts $Cu(ClO_4)_2$ and $Cu(NO_3)_2$ as the Cu^{II} source (Figure S5). Using Milli-Q ultrapure water (> 18 MΩ) or deionized water and solution deaeration with N_2 or Ar had no effect. Replacing Na_2CO_3 with K_2CO_3 gave similar results. These results suggest that the catalytic activity is intrinsic and not due to an impurity in the Cu^{II} source, water, or electrolytes. Cu^{II} water oxidation catalysis was also observed at other electrodes, such as ITO (ITO = Sn^{IV}-doped In_2O_3) or FTO (FTO = fluorine-doped SnO_2; Figure 1c), and glassy carbon (Figure 1d), but the CV profiles at these electrodes are less well defined and the catalytic current densities are smaller.

A large surface area ITO (0.70 cm^2) electrode was used for controlled potential electrolysis at 1.30 V, an overpotential of ca. 700 mV, with $CuSO_4$ (3 mM) in Na_2CO_3 solution (1M, pH = ca. 10.8; Figure 2a). The background for O_2 production at the applied potential was minimal. With added Cu^{II}, catalysis was sustained for at least 6 h at stable current density levels of ca. 2.5 mA cm^{-2}. During the electrolysis, there was a slight current enhancement (ca. 15%) in the initial 20 min, which is probably due to a contribution from a slowly formed, catalytically active surface precipitate (see below). By contrast, the current density in the absence of Cu^{II} was ca. 0.022 mA cm^{-2}. Measurement of oxygen evolved by gas chromatographic analysis (Varian 450-GC; Figure 2b), gave

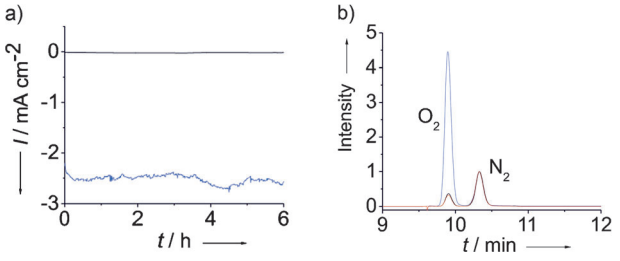

Figure 2. a) Controlled potential electrolysis without (black) and with (blue) 3 mM $CuSO_4$ at an ITO (0.70 cm^2) electrode in Na_2CO_3 solution (1 M, pH = ca. 10.8) at 1.30 V vs. NHE. b) As in (a), gas chromatographic traces in the absence (black) and presence (blue) of $CuSO_4$, and before electrolysis (red). The chromatographic response for O_2 was normalized to residual O_2/N_2 from ambient air. Temperature = 22 °C.

95 μmol of O_2 over an electrolysis period of 6 h with a Faradaic efficiency of 97% for O_2 production through ca. 16 catalytic turnovers, based on Cu^{II} in solution. There was no noticeable change in the UV/Vis spectrum for Cu^{II} during the electrolysis (Figure S6). Under identical conditions, the BDD electrode was more active than an ITO electrode of comparable surface area by a factor of ca. 3.5, with current density reaching ca. 9 mA cm^{-2} for the former.

During long term electrolysis experiments, there was visible evidence of the formation of a precipitated film or solid on the optically transparent ITO electrode, this substance showed absorption features at $\lambda_{max} = 360$ nm and 530 nm (Figure S7). The precipitated solid redissolves in Na_2CO_3 solution (1M, pH 10.8), returning to Cu^{II} within 10–15 min (more rapidly with agitation; Figure S7), but is stable in non-buffered salt solutions such as $NaClO_4$, Na_2SO_4, and $NaNO_3$ (1M, pH adjusted to 10.8 by NaOH), or in pure water. The surface-bound solid is active toward water oxidation in Na_2CO_3 solution (1M, pH 10.8), which adds to the overall catalytic current during sustained water oxidation (Figure S8). These observations are reminiscent of the appearance of catalytically active metal oxide films for other transition metals such as Co, Ni, Mn, and Ir.[7–10,13,15] Scanning electron microscopy (SEM) and X-ray photoelectron spectroscopy (XPS) measurements confirmed that the deposited amorphous solid contains copper and oxygen (Figure S9). Carbon content was negligible compared to the carbon background.

During long term electrolysis in Na_2CO_3 solution (1M), the surface precipitate appeared only at high initial concentrations of Cu^{II}. With a Cu^{II} loading of 1 mM or lower, there was no XPS or SEM evidence for precipitation or film buildup, even after 24 h of sustained electrolysis. These observations point to the concentration dependent, surface equilibrium formation of a higher oxidation state solid or film on the electrode that is electroactive toward water oxidation.

Water oxidation catalysis also occurs in $NaHCO_3$ solution (1M, pH = ca. 8.2) or a $NaHCO_3$ solution saturated with 1 atm CO_2 (0.1M, pH = ca. 6.7). These are relevant conditions for CO_2 reduction in solar fuel applications such as CO_2 splitting ($CO_2 \rightarrow CO + {}^1/_2\,O_2$) where the half reactions are $H_2O - 2e^- \rightarrow {}^1/_2\,O_2 + 2H^+$ and $3CO_2 + H_2O + 2e^- \rightarrow CO + 2HCO_3^-$.[26] In a $NaHCO_3$ solution saturated with 1 atm CO_2 (0.1M, pH = ca. 6.7), the solubility of Cu^{II} is ca. 1.2 mM. Under these conditions, the catalytic current density for water oxidation at ca. 1.65 V and 10 mV s^{-1} varies linearly with $[Cu^{II}]$ to the limit of solubility of $CuSO_4$ (ca. 1.2 mM; Figure 3). This observation is consistent with single site Cu^{II} catalysis, in contrast to di-copper catalysis in Na_2CO_3 solution (1M, pH = ca. 10.8), but the catalytic current density is ca. 6.5-fold lower in the former with Cu^{II} (1 mM) in both cases. Under these conditions, water oxidation appears to be kinetically well behaved through multiple CV scans (Figure S10). At scan rates of ≥ 500 mV s^{-1}, there is evidence for a re-reduction wave at $E_{p,c}$ = ca. 1.25 V. At scan rates of ≤ 20 mV s^{-1}, a scan rate independent catalytic current peak/plateau is apparent at $E_{p,a}$ = ca. 1.65 (Figure S11).

Under these conditions, sustained water oxidation catalysis also occurs at ITO, FTO, and glassy carbon electrodes

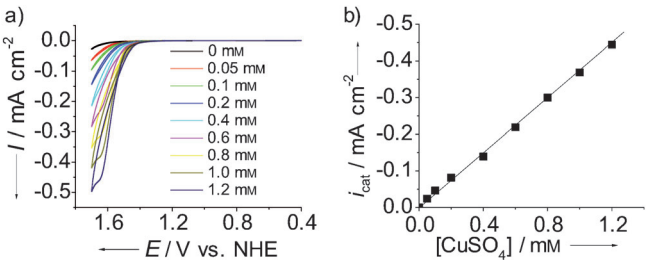

Figure 3. a) CVs of different concentrations of $CuSO_4$ in a $NaHCO_3$ solution saturated with 1 atm CO_2 (0.1 M, pH = ca. 6.7). Electrode = BDD, scan rate = 10 mV s^{-1}. b) Plot of the catalytic current density at 1.65 V vs. NHE against [Cu^{II}]. Temperature = 22 °C.

(Figure S10). Gas chromatographic analysis gave a Faradaic efficiency of 96% for O_2 production over an electrolysis period of 3 h at 1.55 V at the ITO electrode (Figure S12). There was no evidence for the buildup of a film or precipitate during CV scans or long term electrolysis experiments.

In $NaHCO_3$ solution (1M, pH = ca. 8.2), there is qualitative evidence for the involvement of both single site and di-copper catalysis. As can be seen from the data in Figure S13, a new wave appears at 1.55 V at [Cu^{II}] ≥ 4 mM. The current response at 1.55 V is dominated by di-copper catalysis at 4–10 mM, which is the limit of $CuSO_4$ solubility. Below this concentration, single-site catalysis dominates. The competition between the two pathways is also seen in the scan rate dependent CVs, with the di-copper pathway dominating at the expense of the single site pathway at slower scan rates (Figure S14).

The choice of buffer/electrolyte in the appropriate pH domains for water oxidation is critical for Cu^{II}-catalyzed water oxidation to avoid precipitation and maximize the concentration of catalyst. Catalytic water oxidation in a 0.1M solution of $NaNO_3/HNO_3$ or $LiClO_4/HClO_4$ at pH = ca. 6.7 is negligible, which points to an essential role for the proton-accepting/coordinating buffer anions, HCO_3^-/CO_3^{2-}. Increasing the pH without buffer anions results in the precipitation of $Cu(OH)_2$ with $K_{sp}(Cu(OH)_2)$[27] = 2.2×10^{-20}. In spite of the high pH in HCO_3^-/CO_3^{2-} buffered solutions and $K_{sp}(CuCO_3)$[27] = 1.4×10^{-10}, Cu^{II} salts dissolve in Na_2CO_3 (1M, pH = ca. 10.8) which is attributable to coordination and complex formation by HCO_3^-/CO_3^{2-}. A decrease in the concentration of Na_2CO_3 added to 0.1M decreases the solubility of Cu^{II} to < 0.5 mM and the catalytic current density decreases accordingly.

Evidence for bicarbonate/carbonate coordination to Cu^{II} in aqueous $CO_2/HCO_3^-/CO_3^{2-}$ solutions appears in UV/Vis measurements (Figure S15 and S16). The extent of the blue shift in $CO_2/HCO_3^-/CO_3^{2-}$ aqueous solutions at different pHs in Figure S15 is consistent with the coordination by CO_3^{2-} that is dominant at high pH and the coordination by HCO_3^- that is dominant at low pH. A calculated speciation diagram for the ternary Cu^{II}-bicarbonate/carbonate system[28] is consistent with this conclusion, although it was modeled at much lower Cu^{II} (10^{-9} M) and carbonate ($f(CO_2) = 10^{1.5}$ Pa) concentrations. Based on the results of an earlier pulsed electron paramagnetic resonance (EPR) study,[29] the dominant species in solutions which are closer to the catalytic conditions are monodentate/bidentate complexes with HCO_3^-/CO_3^{2-} as ligands; depending on the pH, the remaining coordination sites are occupied by aqua or hydroxo ligands. The presence of aqua or hydroxo ligands is, no doubt, an important feature for water oxidation catalysis and probably provides access to high-oxidation-state Cu-oxo intermediates as sites for O–O coupling, as found for single site polypyridyl Ru[1–4] and Ir[5–7] complexes. As shown in Figure 4, the catalytic current density decreases with further increases in added carbonate, possibly because of complete coordination by carbonate/bicarbonate. The choice of a 1M solution of Na_2CO_3 represents a balance between the enhanced solubility of added Cu^{II} salts and the reactivity of the dominant forms in solution.

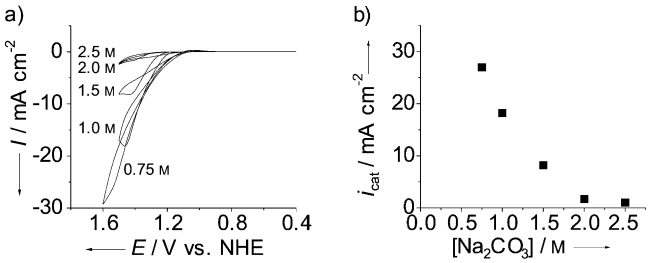

Figure 4. a) CVs of $CuSO_4$ (3 mM) in solutions of different concentrations of Na_2CO_3 (pH = ca. 10.8). Electrode = BDD (0.071 cm^2), scan rate = 100 mV s^{-1}. The ionic strength was kept constant by adding Na_2SO_4. At [Na_2CO_3] < 0.75 M, $CuSO_4$ (3 mM) is insoluble. b) Plot of catalytic peak/plateau current density i_{cat} against [Na_2CO_3]. Temperature = 22 °C.

Catalytic water oxidation also occurs in HPO_4^{2-}/PO_4^{3-} buffered solutions. With added phosphate buffers (0.1M) at pH > 5.0, the precipitation of $Cu_3(PO_4)_2$ dominates with $K_{sp}(Cu_3(PO_4)_2)$[27] = 1.40×10^{-37}. Increasing the phosphate buffer concentration to its solubility limit of ca. 0.8 M at pH = ca. 10.8 increases the solubility of Cu^{II} to ca. 3 mM owing to HPO_4^{2-}/PO_4^{3-} coordination (Figure S15). Based on the results of an electrochemical study, oxidation catalysis under these conditions is also dominated by a reaction pathway that is second order in Cu^{II} (Figure S17), with catalytic current densities comparable to those in Na_2CO_3 solution (1M, pH = ca. 10.8).

Acetate also coordinates to Cu^{II} (Figure S15) and Cu^{II} solubility is enhanced to > 10 mM in a 0.1M solution of acetic acid/acetate at pH 6.0. Under these conditions, as in a $NaHCO_3$ solution (0.1M) saturated with 1 atm CO_2 at pH = ca. 6.7, catalytic currents are first order in [Cu^{II}] (Figure S18), with no evidence for the buildup of a film or precipitate during long term electrolysis experiments. However, electrocatalytic water oxidation is in competition with acetate oxidation, as shown by the appearance of CO_2 as a co-product by gas chromatographic analysis.

Our experimental observations lead to a number of conclusions:

1) In high concentrations of CO_3^{2-}, Cu^{II} is an effective, stable electrocatalyst for sustained water oxidation, albeit with a relatively high overpotential. Highly reproducible CVs and a catalytic current dependence on [Cu^{II}]^2 point to di-

copper catalysis in solution. That the pathway is second order in [Cu^{II}] points to a possible rate limiting step involving CuO—OCu coupling and μ-peroxide or bis(μ-oxo) bridge formation (Cu-OO-Cu), as found for copper monooxygenases.[24] Well-defined copper peroxide and di-copper μ-peroxide or bis(μ-oxo) complexes are well known.[17–19] At high concentrations of Cu^{II} in carbonate solutions, equilibrium formation of a film/solid on the electrode surface occurs, with the solid also contributing to water oxidation and oxygen evolution.[30]

2) In CO_2-saturated, $NaHCO_3$ solution (0.1M, pH = ca. 6.7), a pathway that is first order in [Cu^{II}] dominates water oxidation reactivity. The first order dependence is reminiscent of oxidation of water by single site polypyridyl Ru[1–4] and Ir[5–7] oxidants such as $[Ru^{V}(Mebimpy)(bpy)(O)]^{3+}$ (Mebimpy = 2,6-bis(1-methylbenzimidazol-2-yl)pyridine, bpy = 2,2′-bipyridine).[1] For the Ru complex, the key O–O bond-forming step occurs by concerted oxygen atom proton transfer (APT) to give a terminal peroxide intermediate, $Ru^{V}{=}O^{3+}\cdots O(H){-}H\cdots OP(O)_2OH^{2-} \rightarrow Ru^{III}{-}OOH^{2+} + H_2PO_4^-$.[1] In $NaHCO_3$ solution (1M, pH = ca. 8.2), there is qualitative evidence for the involvement of both single site and di-copper catalysis. From the data obtained in a $CO_2/HCO_3^-/CO_3^{2-}$ buffer solution from pH 10.8 to 8.2 to 6.7, it is clear that water oxidation catalysis is inhibited by decreasing the pH.

3) UV/Vis spectra and earlier pulsed EPR measurements[29] point to HCO_3^-/CO_3^{2-} coordination in solution, which avoids the precipitation of Cu^{II} as $Cu(OH)_2$ or $CuCO_3$ in neutral and weakly basic media, and may lower potentials for accessing higher-oxidation-state intermediates (Cu^{III} and/or Cu^{IV}) in solution.[31,32]

In summary, we have demonstrated robust and sustained electrocatalytic water oxidation based on simple Cu^{II} salts in neutral to weakly basic aqueous $CO_2/HCO_3^-/CO_3^{2-}$, acetate, or HPO_4^{2-}/PO_4^{3-} buffer solutions. Depending on the conditions, there is evidence for water oxidation catalysis by single site, di-copper, and even interfacial catalysis. Even with the relatively high overpotential for water oxidation, the simplicity of the system and the reaction conditions are appealing and may be of value in electrochemical or photoelectrochemical applications.

Received: September 6, 2012
Revised: October 17, 2012
Published online: November 20, 2012

Keywords: coordination environment · copper · electrocatalysis · water oxidation · water splitting

[1] Z. F. Chen, J. J. Concepcion, X. Q. Hu, W. T. Yang, P. G. Hoertz, T. J. Meyer, *Proc. Natl. Acad. Sci. USA* **2010**, *107*, 7225–7229.
[2] H. W. Tseng, R. Zong, J. T. Muckerman, R. Thummel, *Inorg. Chem.* **2008**, *47*, 11763–11773.
[3] S. Romain, L. Vigara, A. Llobet, *Acc. Chem. Res.* **2009**, *42*, 1944–1953.
[4] D. J. Wasylenko, C. Ganesamoorthy, M. A. Henderson, B. D. Koivisto, H. D. Osthoff, C. P. Berlinguette, *J. Am. Chem. Soc.* **2010**, *132*, 16094–16106.
[5] N. D. McDaniel, F. J. Coughlin, L. L. Tinker, S. Bernhard, *J. Am. Chem. Soc.* **2008**, *130*, 210–217.
[6] J. F. Hull, D. Balcells, J. D. Blakemore, C. D. Incarvito, O. Eisenstein, G. W. Brudvig, R. H. Crabtree, *J. Am. Chem. Soc.* **2009**, *131*, 8730–8731.
[7] D. B. Grotjahn, D. B. Brown, J. K. Martin, D. C. Marelius, M.-C. Abadjian, H. N. Tran, G. Kalyuzhny, K. S. Vecchio, Z. G. Specht, S. A. Cortes-Llamas, V. Miranda-Soto, C. v. Niekerk, C. E. Moore, A. L. Rheingold, *J. Am. Chem. Soc.* **2011**, *133*, 19024–19027.
[8] I. Zaharieva, P. Chernev, M. Risch, K. Klingan, M. Kohlhoff, A. Fischer, H. Dau, *Energy Environ. Sci.* **2012**, *5*, 7081–7089.
[9] M. W. Kanan, D. G. Nocera, *Science* **2008**, *321*, 1072–1075.
[10] M. Dincă, Y. Surendranath, D. G. Nocera, *Proc. Natl. Acad. Sci. USA* **2010**, *107*, 10337–10341.
[11] F. Jiao, H. Frei, *Angew. Chem.* **2009**, *121*, 1873–1876; *Angew. Chem. Int. Ed.* **2009**, *48*, 1841–1844.
[12] Q. Yin, J. M. Tan, C. Besson, Y. V. Geletii, D. G. Musaev, A. E. Kuznetsov, Z. Luo, K. I. Hardcastle, C. L. Hill, *Science* **2010**, *328*, 342–345.
[13] J. J. Stracke, R. G. Finke, *J. Am. Chem. Soc.* **2011**, *133*, 14872–14875.
[14] W. J. Youngblood, S. A. Lee, Y. Kobayashi, E. A. Hernandez-Pagan, P. G. Hoertz, T. A. Moore, A. L. Moore, D. Gust, T. E. Mallouk, *J. Am. Chem. Soc.* **2009**, *131*, 926–927.
[15] J. D. Blakemore, N. D. Schley, G. W. Olack, C. D. Incarvito, G. W. Brudvig, R. H. Crabtree, *Chem. Sci.* **2011**, *2*, 94–98.
[16] S. M. Barnett, K. I. Goldberg, J. M. Mayer, *Nat. Chem.* **2012**, *4*, 498–502.
[17] E. A. Lewis, W. B. Tolman, *Chem. Rev.* **2004**, *104*, 1047–1076.
[18] C. J. Cramer, W. B. Tolman, *Acc. Chem. Res.* **2007**, *40*, 601–608.
[19] L. M. Mirica, X. Ottenwaelder, T. D. P. Stack, *Chem. Rev.* **2004**, *104*, 1013–1045.
[20] W. Harnischmacher, R. Hoppe, *Angew. Chem.* **1973**, *85*, 590–590; *Angew. Chem. Int. Ed. Engl.* **1973**, *12*, 582–583.
[21] V. E. Bondybey, J. H. English, *J. Phys. Chem.* **1984**, *88*, 2247–2250.
[22] P. Kang, E. Bobyr, J. Dustman, K. O. Hodgson, B. Hedman, E. I. Solomon, T. D. P. Stack, *Inorg. Chem.* **2010**, *49*, 11030–11038.
[23] M. Taki, S. Itoh, S. Fukuzumi, *J. Am. Chem. Soc.* **2001**, *123*, 6203–6204.
[24] S. Mahapatra, S. Kaderli, A. Llobet, Y.-M. Neuhold, T. Palanché, J. A. Halfen, V. G. Young, Jr., T. A. Kaden, L. Que, Jr., A. D. Zuberbühler, W. B. Tolman, *Inorg. Chem.* **1997**, *36*, 6343–6356.
[25] There is no straightforward way to obtain rate constants for the di-copper pathway of water oxidation from the electrochemical data, but electrocatalytic current densities are cited where appropriate.
[26] Y. Hori, A. Murata, R. Takahashi, *J. Chem. Soc. Faraday Trans. 1* **1989**, *85*, 2309–2326.
[27] P. Patnaik, *Handbook of Inorganic Chemicals*, **2002**, McGraw-Hill, New York.
[28] K. J. Powell, P. L. Brown, R. H. Byrne, T. Gajda, G. Hefter, S. Sjöberg, H. Wanner, *Pure Appl. Chem.* **2007**, *79*, 895–950.
[29] P. M. Schosseler, B. Wehrli, A. Schweiger, *Inorg. Chem.* **1997**, *36*, 4490–4499.
[30] R. H. Crabtree, *Chem. Rev.* **2012**, *112*, 1536–1554.
[31] L. L. Diaddario, W. R. Robinson, D. W. Margerum, *Inorg. Chem.* **1983**, *22*, 1021–1025.
[32] W. Levason, M. D. Spicer, *Coord. Chem. Rev.* **1987**, *76*, 45–120.

